Hydrol. Earth Syst. Sci. Discuss., 12, 8091–8129, 2015
www.hydrol-earth-syst-sci-discuss.net/12/8091/2015/
doi:10.5194/hessd-12-8091-2015

Hydrology and Earth System Sciences
Discussions
Open Access

Assessing various drought indicators in representing drought in boreal forests in Finland

Y. Gao[1], **T. Markkanen**[1], **T. Thum**[1], **M. Aurela**[1], **A. Lohila**[1], **I. Mammarella**[2], **S. Hagemann**[3], **and T. Aalto**[1]

[1]Finnish Meteorological Institute, P.O. Box 503, 00101 Helsinki, Finland
[2]University of Helsinki, Department of Physics, P.O. Box 48, 00014 Helsinki, Finland
[3]Max Planck Institute for Meteorology, Bundesstr. 53, 20146 Hamburg, Germany

Received: 23 July 2015 – Accepted: 1 August 2015 – Published: 19 August 2015

Correspondence to: Y. Gao (yao.gao@fmi.fi)

Published by Copernicus Publications on behalf of the European Geosciences Union.

Abstract

Droughts can impact on forest functioning and production, and even lead to tree mortality. However, drought is an elusive phenomenon that is difficult to quantify and define universally. In this study, we assessed the performance of a set of indicators that have been used to describe drought conditions in the summer months (June, July, August) over a 30 year period (1981–2010) in Finland. Those indicators include the Standardized Precipitation Index (SPI), the Standardized Precipitation–Evapotranspiration Index (SPEI), the Soil Moisture Index (SMI) and the Soil Moisture Anomaly (SMA). Herein, regional soil moisture was produced by the land surface model JSBACH. While SPI, SPEI, and SMA show a degree of anomalies from the statistical means over a period, SMI is directly connected to plant available water and closely dependent on soil properties. Moreover, the buffering effect of soil moisture and the associated soil moisture memory can impact on the onset and duration of drought as indicated by the SMI and SMA, whereas SPI and SPEI are directly controlled by meteorological conditions.

In particular, we investigated whether the SMI, SMA and SPEI are able to indicate the Extreme Drought affecting Forest health (EDF) in Finland. EDF thresholds for these indicators are suggested, based on the spatially representative statistics of forest health observations in the exceptional dry year 2006. Our results showed that SMI was the best indicator in capturing the spatial extent of forest damage induced by the extreme drought in 2006. In addition, the derived thresholds were applied to those indicators to capture EDF events over the summer months of the 30 year study period. The SPEI and SMA showed more frequent EDF events over the 30 year period, and typically described a higher fraction of influenced area than SMI. In general, the suggested EDF thresholds for those indicators may be used for the indication of EDF events in Finland or other boreal forests areas in the context of future climate scenarios. However, the results have to be interpreted carefully, with due consideration of their different properties and the complexity of drought. Our results would suggest that in order to take appro-

priate precautions to mitigate against possible forest losses, an integrated analysis of projected drought with drought indicators is recommended.

1 Introduction

Droughts are expected to become more frequent and severe under global warming (Sergio et al., 2014; Dai, 2013; Schär et al., 2004; IPCC, 2012). Boreal forests have been recognized as a "tipping element" of the Earth system as they are highly sensitive to climate warming (Lenton et al., 2008). In addition to a reduction in forest productivity (Ciais et al., 2005; Granier et al., 2007), severe drought can lead to tree mortality in boreal forests (Allen et al., 2010; Peng et al., 2011). Disturbance of boreal forests could give rise to further feedbacks to the global climate system, due to the complex interactions between boreal forests and the climate system via the control on energy, water and carbon cycles (Bonan, 2008; Ma et al., 2012).

Drought can be essentially defined as a prolonged and abnormal moisture deficiency (World Meteorological Organization, 2012). However, the cumulative nature of drought, the temporal and spatial variance during drought development, and the diverse systems that drought could impact on, make drought difficult to quantify and define universally (Heim, 2002; Veit et al., 2015). The American Meteorological Society (1997) classifies drought into four categories: meteorological or climatological drought, agriculture or soil moisture drought, hydrological drought, and socio-economic drought. Drought is principally induced by a lack of precipitation. Furthermore, high atmospheric water-demand (i.e. potential evapotranspiration, PET), due to warm temperatures, low relative humidity and changes in other environmental variables, often coincides with the absence of precipitation. Through land–atmosphere interactions, prolonged meteorological drought can further exacerbate soil moisture drought, or even hydrological drought (Mishra and Singh, 2010; Tallaksen and Van Lanen, 2004).

Soil moisture strongly regulates transpiration and photosynthesis for most terrestrial plants, consequently modulating water and energy cycles of the landscape, as well as biogeochemical cycles of the plants (Seneviratne et al., 2010; Bréda et al., 2006). Reduction of tree transpiration at the stand-level induced by the low soil moisture condition has been broadly observed in most tree species (Irvine et al., 1998; Bréda et al., 1993; Clenciala et al., 1998). In recent years, micrometeorological flux networks with intensive ancillary data have greatly supported the investigation of the relationship between drought and carbon fluxes over diverse ecosystems (Grossiord et al., 2014; Krishnan et al., 2006; Welp et al., 2007; Law et al., 2002; Grünzweig et al., 2003). In general, those studies observed a growth reduction in forests as a consequence of drought. In addition, studies have shown that regardless of the frequency, duration and severity of droughts, drought-induced forest damages may be connected to specific soil and plant characteristics, such as soil texture and depth, exposure, species and their composition and life stage (Muukkonen et al., 2015; Grossiord et al., 2014; Dale et al., 2001; Gimbel et al., 2015).

Forest damage induced by drought is a cumulative effect and is closely linked to soil moisture. Nevertheless, most soil moisture drought studies have been conducted at a stand-scale due to the limited observational data in space. Regional analysis is necessary to fully capture the spatial heterogeneity of the impacts of drought on ecosystem functioning (Aalto et al., 2015). In recent years, a multi-decadal global soil moisture record that incorporates passive and active microwave satellite retrievals has become available (Liu et al., 2012). However, microwave remote sensing can only provide surface soil moisture in the upper centimeters of the soil. Land surface models (LSMs) are a valuable tool to derive spatial maps of soil moisture in deeper soil layers, for instance, the root-zone soil moisture which is of particular importance in many climate studies (Hain et al., 2011; Rebel et al., 2012; Seneviratne et al., 2010).

A number of drought indicators have been developed in the past in order to quantify the characteristics of the different drought types and their potential impacts on diverse ecosystems and societies (Heim, 2002). The most prominent and widely used drought indicator is the Standardized Precipitation Index (SPI), which has been recommended as a standard drought indicator by the World Meteorological Organization (WMO) due to its flexibility for various time scales, simplicity in input parameters and calculation, as well as effectiveness in decision making (Sheffield and Wood, 2011; Hayes et al., 2011). The SPI was developed to provide a spatially and temporally invariant comparison of drought determined by precipitation at different time scales (McKee et al., 1993, 1995). The Standardized Precipitation–Evapotranspiration Index (SPEI) is developed based on the SPI, and, in addition to precipitation, also accounts for temperature impacts on drought (Vicente-Serrano et al., 2010). Soil moisture status has been explored through the Soil Moisture Anomaly (SMA) and Soil Moisture Index (SMI). The SMA has been adopted in the Coupled Model Intercomparison Project (CMIP) in order to study soil moisture drought in present and future projections in Global Circulation Models (GCMs) (Orlowsky and Seneviratne, 2013). The SMI (also referred to as Relative Extractable Water (REW)) is often used to investigate soil water related plant physiology issues, as it can represent the relative plant available water in the root zone (Lagergren and Lindroth, 2002; Granier et al., 1999).

In this study, we assessed the performance of several drought indicators (SPI, SPEI, SMA and SMI) for their ability to capture the timing and spatial extent of droughts in Finland. In particular, we examined the effectiveness of the indicators to capture the extreme drought that took place in Finland in 2006, and which caused visible impacts on forest appearance. The damaged forest sites were mainly located in southern Finland during the 2006 drought, and 24.4 % of the forest health observational sites over entire Finland (total number of sites = 603) were affected, in contrast to 2–4 % damaged sites in a normal year (Muukkonen et al., 2015). This information was then used to determine indicator thresholds for Extreme Drought affecting Forest Health (EDF). Based on the derived indicator thresholds, the EDFs for the summer months of a 30 year period (1981–2010) in Finland were indicated. In addition, the soil moisture based drought indicators (SMA, SMI) were derived from the regional soil moisture, which was simulated by the JSBACH LSM with its updated soil hydrology scheme. Thus, this study also aims to gain insights into the capability of the updated soil hydrology scheme with its parameters in the JSBACH LSM to simulate soil moisture dynamics across Finland.

HESSD
12, 8091–8129, 2015

2 Data and methods

2.1 Study area

Our study area is focused on Finland (Fig. 1). Finland is a northern European country, situated between 60 and 70° N in the northwestern part of the Eurasian continent, close to the North Atlantic Ocean. The coastline of Finland borders the Baltic Sea, the Gulf of Bothnia, and the Gulf of Finland. There are many inland lakes in Finland, especially in the southeastern part of the country. The highest points in Finland appear in the Scandinavian mountain range in northern Lapland, reaching an elevation of around 1000 m a.s.l. The rest of Finland shows only small variations in elevation, thereby favoring the development of wetlands and the formation of peat. The topography in these areas is less than 300 m a.s.l.

Climatic features in Finland follow the geographical characteristics of the region. The westerly winds bring warm air masses from the North Atlantic Ocean in winter, while in summer they bring clouds that decrease the amount of incoming solar radiation. Therefore, the temperature of Finland is generally moderate, compared to many other places at the same latitudes (Tikkanen, 2005). However, the continental high pressure system located over the Eurasian continent occasionally influences the climate causing warm and cold spells in summer and winter, respectively. The precipitation in Finland is influenced by the Scandinavian mountain range, which blocks large amounts of moisture that are transported from west to east. Both temperature and precipitation show spatial variations along a south to north gradient. The annual mean surface temperature is about 5–6 °C in the south of Finland and extends below −2 °C in the coldest area located in northern Lapland. Annual precipitation, averaged over the 1971–2000 period, is more than 700 mm in the south and less than 400 mm in the north (Aalto et al., 2013; Drebs et al., 2002).

The soil types in Finland mainly include mineral soils and peat. Peatland coverage is higher in northern Finland. The shallow soil areas are mostly located around the

HESSD
12, 8091–8129, 2015

coastline in southern Finland because of a high proportion of bare rock areas, and are also found in north-west Finland, which is a part of the Scandinavian mountain range.

Coniferous forest, including Scots pine and Norway spruce, is the dominant forest type in Finnish boreal forests (Finnish Statistical Yearbook of Forestry 2012, 2012). Broadleaved forest accounts for less than 10 % of the forest area. 75 % of the total forest land area is located on mineral soils. Moreover, as a result of the originally high proportion of pristine peatlands and timber production requirements, large areas of unproductive peatlands have been drained to grow forests in Finland in the past (Päivänen and Hånell, 2012).

2.2 Observational data

The gridded meteorological data compiled by the Finnish Meteorological Institute (FMI gridded observational data) are interpolated products from stand meteorological observations in Finland (Aalto et al., 2013). In this study, daily FMI gridded observational data were used on a 0.2° longitude × 0.1° latitude grid for the period 1981–2010. These data comprise daily mean, minimum and maximum temperatures, precipitation, relative humidity, and incoming shortwave radiation. In addition, the 10 m wind speed of ECWMF ERA-Interim reanalysis data (Simmons et al., 2007) was used to calculate the reference evapotranspiration (ET_0) for SPEI from the Penman–Monteith equation (Allen et al., 1998).

In addition, meteorological and soil moisture data at three micrometeorological sites were used as meteorological forcing for site level simulations and for a comparison of modelled and observed soil moisture, respectively (Fig. 1; Table 1). Soil parameters derived from observations are only available for the Hyytiälä site (water content at saturation (θ_{SAT}) = 0.50 $m^3\,m^{-3}$, water content at field capacity (θ_{FC}) = 0.30 $m^3\,m^{-3}$, water content at wilting point (θ_{WILT}) = 0.08 $m^3\,m^{-3}$). As explained in more detail below, we used the second layer of simulated soil moisture in the JSBACH soil profile (layer-2; 6.5–30 cm). Therefore, the observed soil moisture data were taken from existing measurement depths, which are consistent with the JSBACH layer-2 soil depth. For

HESSD
12, 8091–8129, 2015

the Sodankylä site, an average of the measurements at soil depths −10, −20 and −30 cm was employed and for the Kenttärova site, the measurement at −10 cm was used. The two levels in the Hyytiälä soil moisture measurement, −5 to −23 and −23 to −60 cm, were both used.

2.3 JSBACH land surface modelling

JSBACH (Brovkin et al., 2009; Raddatz et al., 2007) is the land surface scheme (LSS) of the Max Planck Institute for Meteorology Earth System Model (MPI–ESM) (Stevens et al., 2013; Roeckner et al., 1996). It simulates energy, hydrology and carbon fluxes in response to climate drivers. In the original bucket scheme for soil hydrology, the maximum water can be stored in the soil moisture reservoir (W_{cap}), which corresponds to the root zone water content (Hagemann, 2002). The bucket can be supplied from precipitation and snow melt, but depleted through evapotranspiration (evaporation from the upper 10 cm of soil and plant transpiration from below), and lateral drainage. These processes are related to the amount of soil moisture in the bucket and are regulated by the Arno scheme, which separates rainfall and snow melt into surface runoff and infiltration, and considers soil heterogeneity (Dümenil and Todini, 1992).

In order to more adequately simulate the soil hydrology, a five layer soil moisture scheme has been introduced in JSBACH (Hagemann and Stacke, 2015). The five layer structure is defined with increasing layer thickness (0.065, 0.254, 0.913, 2.902, and 5.7 m) and reaches almost 10 m depth below the surface. However, the soil depth to the bed rock, determines the active soil layers. Therefore, in the updated soil hydrology scheme, the root zone is differentiated into several layers, and there could be soil layers below the root zone, which transport water upwards for transpiration when the root zone has dried out. Moreover, evaporation from bare soil can occur when the uppermost layer is wet, while the whole soil moisture bucket must be largely saturated in the bucket scheme. For a more detailed description of the improved soil hydrology scheme in JSBACH and how it affects soil moisture memory, see Hagemann and Stacke (2015).

HESSD
12, 8091–8129, 2015

In this work, the regional JSBACH simulation was driven by the prescribed meteorological data (1980–2011) simulated by the regional climate model REMO (Jacob, 2001; Jacob and Podzun, 1997), whose biases of modelled temperature and precipitation were corrected with the FMI gridded observational data (Aalto et al., 2013). A quantile–quantile type bias correction algorithm was applied to daily mean temperature (Räisänen and Räty, 2013), while daily cumulative precipitation was corrected using parametric quantile mapping (Räty et al., 2014). The ECWMF ERA-Interim reanalysis (Dee et al., 2011) was used as lateral boundary data for the atmospheric variables and as the initial values of surface variables for the REMO simulation. Both the regional JSBACH and REMO simulations were conducted in the Fennoscandian domain centered on Finland with a spatial resolution of 0.167° (15–20 km). The land cover distribution over this domain was derived from the more up-to-date and more precise Corine land cover 2006 data (European Environment Agency, 2007) rather than the standard GLCCD (US Geological Survey, 2001), which is important for simulating land–atmosphere interactions (Gao et al., 2015; Törmä et al., 2015). As shown in Fig. 1, an improved FAO (Food and Agriculture Organization of the United Nations) soil type distribution is adopted in the JSBACH LSM (FAO/UNESCO, 1971–1981, see Hagemann and Stacke, 2015, for details), while the soil depth distribution is derived from the soil type dataset and FAO soil profile data (Dunne and Willmott, 1996).

In addition, simulations were carried out for the three measurement sites with the observed local meteorological forcing and one plant functional type to describe the vegetation of the site. The characteristics of the sites together with the corresponding model settings are described in Table 1.

Prior to the multi-year JSBACH production runs, a 30 year run was conducted for both the regional and the site level simulations by cycling meteorological forcing to obtain equilibrium for the soil water and soil heat balances.

HESSD
12, 8091–8129, 2015

2.4 Drought indicators

A set of hydro-meteorological indicators were analyzed. The SPI, SPEI and SMA were calculated with 4 weeks (28 days) running mean inputs over the 30 year period. Both are considered to be of sufficient duration climatologically under WMO guidelines (World Meteorological Organization, 2012). The SMI was calculated daily. SPI and SPEI were calculated using both the regional observational dataset and the regional JSBACH forcing data, while SMA and SMI were computed with the layer-2 soil moisture from the regional JSBACH simulation. In addition, the SMIs were derived from site soil moisture observations, as well as from site JSBACH simulations. The layer-2 soil moisture from the JSBACH simulations was used, because the soil moisture in the shallower layer (layer-1) is highly sensitive to small changes in climatic variables, and the soil moisture dynamics in the deeper layers are excessively suppressed. Furthermore, the layer-2 is representative of the root zone in forest soils.

2.4.1 Soil Moisture Index (SMI)

The SMI is a measure of plant available soil water content relative to the maximum plant available water in the soil (Betts, 2004; Granier et al., 2007; Seneviratne et al., 2010). The soil water above field capacity cannot be retained, and produces gravitational drainage and usually flows laterally away. The soil water below the wilting point is strongly held by the soil matrix to such an extent that the plants are unable to overcome this suction to access the water (Hillel, 1998).

The SMI is calculated as follows:

$$\mathrm{SMI} = (\theta - \theta_{\mathrm{WILT}})/(\theta_{\mathrm{FC}} - \theta_{\mathrm{WILT}}),$$

where θ is the volumetric soil moisture [$\mathrm{m^3_{H_2O}\,m^{-3}_{soil}}$], θ_{FC} is the field capacity, θ_{WILT} is the permanent wilting point.

Note that soil water content can exceed θ_{FC} and reach water-holding capacity (i.e. saturation ratio) under certain circumstances. For those cases, the SMI is set to 1,

HESSD
12, 8091–8129, 2015

indicating maximum plant available water. θ_{FC} and θ_{WILT} depend on soil types in this study, although θ_{WILT} is also related to PFTs in some other studies. At Hyytiälä, θ_{SAT} (saturation ratio) was used instead of θ_{FC} to be consistent with the JSBACH soil hydrology where θ_{FC} acts as a proxy for θ_{SAT} on the large ESM grid scale (Hagemann and Stacke, 2015).

2.4.2 Soil Moisture Anomaly (SMA)

The SMA is an index relevant to plant functioning (Burke and Brown, 2008). The SMA depicts the deviation of the soil moisture status in a certain period of a year to the soil moisture climatology over this period. It can be normalized by the standard deviation of the soil moisture in this respective period over all years, for direct comparison with the other standardized drought indicators, e.g. SPI, SPEI.

The SMA in this study is calculated following the method of Orlowsky and Seneviratne (2013):

$$\mathrm{SMA} = \left(\overline{\theta} - \overline{\mu}\right) / \overline{\sigma},$$

where $\overline{\theta}$ denotes the averaged volumetric soil moisture over a certain period in a year, while $\overline{\mu}$ and $\overline{\sigma}$ denote the mean and standard deviation of the volumetric soil moisture of this period over all the studied years.

2.4.3 Standardized Precipitation Index (SPI)

The SPI inspects the amplitudes of precipitation anomalies over a desired period with respect to the long-term normal. The homogenized precipitation series is fitted into a normal distribution to define the relationship of probability to precipitation (Edwards and McKee, 1997). In this work, a Pearson Type III distribution is adopted because it is more flexible and universal with its three parameters in fitting the sample data than the two parameter Gamma distribution (Guttman, 1994, 1999). Typically, the timescales of

HESSD
12, 8091–8129, 2015

SPI range from 1–24 months. The reduced precipitation under various durations can illustrate the impacts of drought on different water resources (Sivakumar et al., 2011). A time frame of less than 1 month is not recommended as the strong variability in weekly precipitation may lead to erratic behavior in the SPI (Wu et al., 2007). However, the "moving window" of a minimum of 4 weeks with daily updating is acceptable (World Meteorological Organization, 2012). Furthermore, attention should be paid when interpreting the 1 month SPI to prevent misunderstanding. Large values in the 1 month SPI can be caused by relatively small departures from low mean precipitation (World Meteorological Organization, 2012).

The SPI is a probabilistic measure of the severity of a dry or wet event. An arbitrary drought classification with specific SPI thresholds was defined by McKee et al. (1993). Recently, an objective method based on percentiles from the United States Drought Monitor (USDM) has been recommended for defining location-specific drought thresholds (Quiring, 2009).

2.4.4 Standardized Precipitation–Evapotranspiration Index (SPEI)

The SPEI is similar to SPI, but also accounts for the impact of temperature on drought through PET, in addition to the water supply from precipitation (Vicente-Serrano et al., 2010). The climatological surface water balances, normalized by the Log-logistic probability distribution over the analysis period, are used to derive SPEI. In this work, PET was calculated according to the FAO-56 Penman–Monteith equation (Allen et al., 1998), which is predominately a physical-based method and has been tested over a wide range of climates (Ventura et al., 1999; López-Urrea et al., 2006).

HESSD
12, 8091–8129, 2015

3 Results and discussion

3.1 Comparison of site soil moisture from JSBACH simulations with observations

The SMI series at the three study sites from the site and the regional (the model grids where the sites are located) JSBACH simulations were compared with the observed soil moisture data over the common data coverage periods (Fig. 2). SMI based on the Hyytiälä observational data was calculated with θ_{SAT} and θ_{WILT} values measured at the site. Due to the lack of soil parameters at the Sodankylä and Kenttärova sites, the volumetric soil moisture measurements were directly used to examine the simulated soil moisture dynamics. An upper limit was set on the presented volumetric soil moisture to exclude abrupt and instantaneous peaks due to heavy snow melting or precipitation.

Simulated soil moisture corresponded well with the observations in describing the timing of dry spells in summer in most of the years at the three sites. Moreover, there was good agreement between the minimum values reached by the simulated and observed SMIs in summertime at Hyytiälä. The late summer of 2006 was noticeable as being extremely dry in the simulations and observations at Hyytiälä and Sodankylä. At Kenttärova, the extent of the SMI was quite different in the regional and site JSBACH simulations. This was mainly because different soil types are prescribed for this site, which affects not only the soil hydrology but also the values of SMI. In the regional simulation, Kenttärova was situated in a peat soil area, while in reality and in the site simulation the site is classified within a mineral soil area. The soil type in an individual grid for the regional simulation is defined according to the soil type with the highest coverage. The summer of 2009 was the driest among the three years at Kenttärova, and the timing of the driest period in late summer shown in the observations was successfully captured by both site and regional simulations. Moreover, the soil at Kenttärova was unsaturated during those three years, even in the site simulations where it was realistically represented as a mineral soil. This could be related to the small amount of precipitation during those years.

HESSD
12, 8091–8129, 2015

Furthermore, the diverse features of soil moisture among these sites in wintertime were captured by JSBACH. The soil tends to be saturated at Hyytiälä in winter, whereas at Sodankylä and Kenttärova there is a winter recession period of soil moisture when the soil tends to dry out. At Hyytiälä, the difference is due to infiltration of snowmelt water during intermittent periods when air temperature is above 0 °C, while at Sodankylä and Kenttärova, periods when the surface soil is frozen are more persistent and only percolation takes place then. The exceptionally low soil moisture during the winter 2003–2004 was also well simulated for Hyytiälä. This winter dry spell was caused by low rainfall in autumn 2003 and the relatively cold winter afterwards when there was not enough snowmelt water to recharge the deficit volume. This autumn-to-winter drought in 2003 at Hyytiälä was a rain to snow season drought (a precipitation deficit in the rainy season and at the beginning of the snow season) in combination with a cold snow season drought (Van Loon and Van Lanen, 2012). The winter recession period of soil moisture at Kenttärova is longer than that in Sodankylä, probably because Kenttärova is located at higher latitudes. Large and obvious decreases in soil water immediately after the winter recession periods of soil moisture in 2008 and 2009 were shown by the site simulation, but not by the regional simulation. This is due to less precipitation during this period in the meteorological forcing data for the site simulation, in comparison to the regional simulation (data not shown). Moreover, the balance between water consumption through evapotranspiration and water gained from snow melt was more negative in the site simulations. In general, the layer-2 soil moisture in the regional simulation for Kenttärova, captures the observed soil moisture dynamics at −10 cm depth better. However, a full evaluation would require observational data from several closely spaced soil layers.

Overall, there is a good agreement with respect to the seasonal dynamics between simulated and observed soil moisture, although the simulated soil moisture shows larger amplitudes and a faster response to changes in water inputs. The discrepancies in soil moisture between the site and the regional JSBACH simulations are mainly due to the differences in precipitation in summertime and in surface temperature during winter in the meteorological forcing data, as well as different soil types in specific locations. The latter is related to the difference in scales between the regional grid and the site. Soil characteristics tend to be heterogeneous, so that the characteristics may vary on scales from a meter to a kilometer. While for modelling on the regional grid, effective soil characteristics are chosen that represent the average characteristics of a gridbox.

3.2 Comparison of drought indicators

The time correlations over our study period between the SPI calculated with the observational dataset and the SPI calculated with the JSBACH forcing data were derived for the gridboxes in Finland. The same approach has been adopted for the SPEIs. Moreover, the time correlations between the meteorological based drought indicators (SPI, SPEI) calculated with the JSBACH forcing data and the soil moisture based drought indicators (SMI, SMA) calculated with the JSBACH simulated soil moisture were derived for the gridboxes in Finland, as well as the time correlation between SMI and SMA (Fig. 3). In general, high correlation coefficients were found throughout Finland. The medians of the time correlation coefficients over the whole of the country were greater than 0.6; with the 5 % percentiles also greater than 0.5, with the exception of the correlation coefficient between SMA and SPI. The agreement between SPEIs calculated with the JSBACH forcing data and the observational dataset was better than that for SPIs. Furthermore, the soil moisture based drought indicators revealed a better correspondence with SPEI than with SPI, which is reasonable as SPEI is based on the water balance. Therefore, in the following, we will focus on SPEI as the climatic driver indicator, and as there was a good correlation between the JSBACH forcing data and the observational data based SPEIs, we restricted the dataset by using the JSBACH forcing data based SPEI, which was better related to the two soil moisture based drought indicators from the model. Moreover, the correlation between SPEI and daily SMI was higher than that between SPEI and SMA. This is especially true for peatland areas while the correlations in mineral soil areas are more similar (data not shown). This may be a result of differing soil moisture memory effects in those soil types.

The spatial and temporal evolution of drought depicted by the selected indicators was compared through time–latitude transections (Fig. 4). The most exceptional dry years in our study period (e.g. 1994, 2006) can be distinguished in all three indicators, as well as the exceptionally wet years (e.g. 1981, 1998). Although there is generally a good correlation among all three indicators in capturing drought, there are differences among them in depicting drought durations and latitudinal extent at detailed locations and time. Firstly, SPEI and SMA generally show more consistent patterns extending through a wider range of latitudes than SMI. Also, the buffering effect of soil moisture and the associated soil moisture memory can delay and extend dry or wet events as indicated by SMI and SMA, in comparison to those by the SPEI. For instance, the dry period in 1992 over southern Finland in SMI and SMA is longer than that in SPEI, and the wet period in the same year over northern Finland as indicated by SMA starts later in comparison to SPEI, however this difference is not shown by SMI. Secondly, SMI exhibits a more distinct south–north gradient than the other two indicators. In particular, SMI describes more frequent droughts in the extreme southern parts of Finland. This is because the shallow soil in those areas is more sensitive to climate drivers. However, there is much less drought indicated by SMI in the extreme northern part of the country (above 68° N). This could be due to the atmospheric water demand at the same SPEI drought level in the north is weaker than that in the south. In other words, the deviation of the multi-year mean value in precipitation surplus (precipitation – evapotranspiration) can lead to a relatively higher change in SPEI values in the very north of Finland than in the south, as the variability of the climate in the north of Finland is lower. Thirdly, SMI between latitudes 66 and 68° N shows an evident narrow range, i.e. the soil is not saturated or deeply dried out. This is due to the abundance of peatland areas with a larger soil moisture buffer than mineral soil areas.

SMI values vary within different ranges for the two soil types in southern and northern Finland, whereas SMA and SPEI show no differences regarding the soil type or location

HESSD
12, 8091–8129, 2015

as they are standardized indicators (Fig. 5). The regionally averaged SMI over the peatland areas mainly varies from 0.4 to 0.6 in both the south and north of Finland, while the SPEI averaged over the same area ranges between −2.0 and 2.0. SMI in the mineral soil shows larger variations compared to peat soil under the same climatic conditions. The SMI averaged over the mineral soil areas ranges between 0.1 and 1.0 in the south of Finland and 0.4 to 1.0 in the north of Finland. The higher values associated with the regionally averaged SMI in the north are due to less shallow soils and less meteorological drought in comparison to the south.

3.3 Extreme Drought that affects Forest health (EDF) indicated by drought indicators

According to the forest health observation data, the forest sites that showed drought damage symptoms in the severe drought in 2006 were mainly located in southern Finland. The proportion of the damaged forest sites reached 30 % in southern Finland (Muukkonen et al., 2015). Herein, we consider this fraction of sites as the fraction of the area influenced by drought, which is a reasonable assumption based on the dense and even distribution of observation sites over southern Finland. Based on this information, we utilized the cumulative area distributions of the SMI and SMA over southern Finland during the driest 28 day period of southern Finland in 2006 (i.e. in the case of SMI, this is the lowest 28 day running mean value averaged over southern Finland) to derive indicator thresholds for this kind of extreme drought (Fig. 6). Herein, as SMA was calculated with 28 day running means for soil moisture, the same time window was adopted for SMI to be consistent with SMA.

Our results showed that the driest 28 day periods of southern Finland in 2006 were the same (from 20 July to 16 August) for SMI and SMA. The SMI and SMA thresholds for the EDF are 0.138 and −2.287, respectively. Moreover, according to the recommended percentile classification (Quiring, 2009), the SPEI threshold for extreme drought, which is selected as 2 % of the SPEI data series, is −1.85 averaged over the gridboxes in Finland (–1.843 averaged over Southern Finland). The averaged SPEI values over the EDF influenced areas in Finland depicted by SMI and SMA for the same period are −1.84 and −1.89, which are very close to the percentile dependent SPEI threshold for extreme drought. This demonstrates that the degrees of EDF described by the derived SMI and SMA thresholds are consistent with the percentile based threshold of extreme drought for SPEI, which is taken as the EDF threshold for SPEI.

Furthermore, we compared the regional distributions of the areas influenced by the 2006 EDF in the driest 28 day period indicated by SMI, SMA and SPEI (Fig. 7). The SMI showed that the EDF influenced areas were mainly located in southern Finland, whereas the SMA showed more EDF affected areas located in the middle to northern part of the country (mainly above 64° N). The EDF influenced areas presented by SMA in the north were mainly located in peatland areas, where the porosity of peat is much higher than that of mineral soils. Although there was a strong decrease in relative soil moisture with respect to the long-term mean value in those areas during this EDF event, the absolute soil moisture for SMI was not sufficiently low for those areas to be recognized as EDF impacted areas (Fig. 5). Moreover, the EDF influenced areas in the southeastern part of Finland, as indicated by SMI, were not shown by SMA, although these areas comprise relatively low SMA values. This is because there were more EDF influenced areas indicated by SMA in the middle of Finland compared to SMI. Those areas took up a part of the 30 % influenced area over the entire southern Finland, which has been used for the selection of EDF thresholds by the cumulative area distributions. The areas impacted by EDF as indicated by SPEI, are widespread over Finland, complying with the climate conditions in this period. The extremely dry climate in northern Finland led to the EDF shown by SMA, but was not sufficiently intense for EDF to be captured by SMI. In southern Finland, the EDF areas of SMI generally agree with those of SPEI, except for the shallow soil area along the southern coastline and in the southeastern part of the country (at 63° N). This more severe drought, which was indicated by SMI rather than by SPEI in the driest 28 day period, points to the vulnerability of shallow soil to climate variability. Also, it is worth noting that the EDF area in the driest 28 day period as indicated by the SMI, shows a similar spatial pattern to the locations of damaged forest sites in the observation data, where few forest damaged sites are found in northern Finland.

A more comparative analysis of the ability of the three indicators to represent EDF under the derived thresholds was conducted for the summer months of the 30 study year period (Fig. 8). As the shallow soil is quite sensitive to climate variation, areas with soil depths less than 3 m were excluded to eliminate the influence on drought period by sporadic drought episodes that would have exaggerated the number of drought days. In general, the drought periods (number of days) influenced by EDF show a better consistency among the three indicators than the mean fraction of affected areas. SMI shows less area under EDFs in both southern and northern Finland than the other two indicators. In particular, the only EDF indicated by SMI in the north was for 2006, but with only a small fractional area of around 1–2 %. In the south, the SMI indicates EDF events in 1994 and 2006, with the mean influenced area larger than 5 % and the period longer than 30 days. In 2006, the mean influenced areas indicated by the SMI and SMA are similar, as are the drought periods. However, the SMA shows less mean influenced areas compared to SMI in 1994. The SPEI displays higher mean areas influenced by EDFs than the soil moisture drought indicators in all years, except 1990. The reason for this is that the EDF as indicated by SPEI in that year had already commenced before June, which is the first month of summer in our study. The SMA shows a prolonged effect in comparison to meteorological drought, which is not sufficiently strong to allow SMI to reach the EDF threshold due to the high initial soil moisture content.

4 Conclusions

This study aims to improve our understanding of the properties of different drought indicators (including SPI, SPEI, SMA and SMI), and their ability to indicate the Extreme Drought that affects Forest health (EDF) in boreal forests in Finland.

The soil moisture based drought indicators (SMA, SMI) were calculated with the regional soil moisture as simulated by the land surface model JSBACH with its updated soil hydrology scheme. Simulated soil moisture was in good agreement with the observed soil moisture data at the three sites with regard to seasonal dynamics of soil moisture and the timing of dry spells, although inconsistencies exist in the rates of change and amplitudes of variations in soil moisture. The discrepancies between site and regional forcing data in precipitation and temperature explain the differences between site and regional simulated soil moisture in summertime and wintertime, respectively.

Moreover, the SPEI showed higher time correlation coefficients with the soil moisture based drought indicators than SPI, as SPEI takes into account the surface water balance rather than precipitation only. Further inspections of the temporal and spatial variability of SPEI, SMA and SMI revealed that, in general, the SPEI and SMA showed latitudinal-consistent patterns, whereas the SMI described more droughts for the south than the north of Finland. This is because SPEI and SMA are both standardized indicators that describe the degrees of anomalies over a period, whereas SMI is directly related to plant available water. The vulnerable shallow soil area along the coastline in southern Finland, and the peat soil area in northern Finland are drought-prone and drought-resistant areas respectively as indicated by SMI. Therefore, soil characteristics impact on SMI. In addition, soil moisture buffering effects and the associated soil moisture memory can delay and extend the drought as indicated by soil moisture based drought indicators, in comparison to those by the SPEI.

The SMI, SMA and SPEI thresholds for EDF were derived as 0.138, −2.287 and −1.85, respectively. The SMI was found to be more capable in spatially representing the EDF in 2006. High discrepancies were found among the indicated EDF periods and the mean fraction of affected areas by the three indicators for the summer months of the 30 year study period. The SPEI was the most sensitive drought indicator and showed the highest amount of EDFs with larger influenced areas, while the SMI showed much less EDF events than the other two indicators. The SMI indicated EDF events in 1994 and 2006 in southern Finland, with the mean affected area larger than 5 % and the period longer than 30 days. Here, the shallow soil areas with a soil depth less than

3 m were excluded. In general, the suggested SMI, SMA and SPEI thresholds for EDF could be adopted to indicate EDF events in Finland or other boreal forests areas under future climate scenarios. However, it is strongly recommended that integrated analyses of drought indicators representing different types of drought should be conducted for future drought projections, in order to ensure the most beneficial drought management decision.

Additionally, drought damage on different tree species could be studied in the future, although this would require more detailed information at the forest observation sites. Moreover, to improve the accuracy of soil moisture based drought indicators (especially SMI) calculated with LSM simulated soil moisture, high quality soil type distribution and soil parameters data are essential. More sophisticated models are expected to improve simulated soil moisture; for instance, soil layers with different soil types along the soil profile, and thorough consideration of the model formulations and parameters that regulate the rate of evapotranspiration, drainage and run-off. Furthermore, uncertainties associated with the drought indicators may originate from their input data (Naumann et al., 2014), therefore unbiased forcing data are of vital importance for the accurate simulation of soil moisture by a LSM (Maggioni et al., 2012).

Acknowledgements. We would like to thank EMBRACE (EU 7th Framework Programme, Grant Agreement number 282672) and HENVI (Helsinki University Centre for Environment) projects for the financial support. We give our deepest appreciation to Pentti Pirinen and Matti Kämäräinen from FMI for providing the observational data. The authors acknowledge MPI–MET, MPI–BGC and CSC (Hamburg) for providing JSBACH and REMO models and assistance in their use, and also the MONIMET project (LIFE12 ENV/FI/000409) for supporting the drought indicator study. This work was also supported by the Academy of Finland Center of Excellence (No. 272041), ICOSFinland (No. 281255) and ICOS-ERIC (No. 281250) funded by Academy of Finland.

HESSD
12, 8091–8129, 2015

References

Aalto, J., Pirinen, P., Heikkinen, J., and Venäläinen, A.: Spatial interpolation of monthly climate data for Finland: comparing the performance of kriging and generalized additive models, Theor. Appl. Climatol., 112, 99–111, 2013.

Aalto, T., Peltoniemi, M., Aurela, M., Böttcher, K., Gao, Y., Härkönen, S., Härmä, P., Kilkki, J., Kolari, P., Laurila, T., Lehtonen, A., Manninen, T., Markkanen, T., Mattila, O.-P., Metsämäki, S., Muukkonen, P., Mäkelä, A., Pulliainen, J., Susiluoto, J., Takala, M., Thum, T., Tupek, B., Törmä, M., and Ali, N. A.: Preface to the special issue on monitoring and modelling of carbon-balance-, water- and snow-related phenomena at northern latitudes, Boreal Environ. Res., 20, 145–150, 2015.

Allen, C. D., Macalady, A. K., Chenchouni, H., Bachelet, D., McDowell, N., Vennetier, M., Kitzberger, T., Rigling, A., Breshears, D. D., and Hogg, E. T.: A global overview of drought and heat-induced tree mortality reveals emerging climate change risks for forests, Forest Ecol. Manag., 259, 660–684, 2010.

Allen, R. G., Pereira, L. S., Raes, D., and Smith, M.: Crop Evapotranspiration-Guidelines for Computing Crop Water Requirements, FAO Irrigation and Drainage paper No. 56, Food and Agriculture Organization of the United Nations, Rome, 1998.

American Meteorological Society: Meteorological drought-policy statement, B. Am. Meteorol. Soc., 78, 847–849, 1997.

Aurela, M., lohila, A., Tuovinen, J.-P., Hatakka, J., Penttilä, T., and Laurila, T.: Carbon dioxide and energy flux measurements in four northern-boreal ecosystems at Pallas, Boreal Environ. Res., 20, 455–473, 2015.

Betts, A. K.: Understanding Hydrometeorology Using Global Models, B. Am. Meteorol. Soc., 85, 1673–1688, doi:10.1175/BAMS-85-11-1673, 2004.

Bonan, G. B.: Forests and Climate Change: Forcings, Feedbacks, and the Climate Benefits of Forests, Science, 320, 1444–1449, doi:10.1126/science.1155121, 2008.

Bréda, N., Cochard, H., Dreyer, E., and Granier, A.: Water transfer in a mature oak stand (Quercuspetraea): seasonal evolution and effects of a severe drought, Can. J. Forest Res., 23, 1136–1143, doi:10.1139/x93-144, 1993.

Bréda, N., Huc, R., Granier, A., and Dreyer, E.: Temperate forest trees and stands under severe drought: a review of ecophysiological responses, adaptation processes and long-term consequences, Ann. For. Sci., 63, 625–644, 2006.

Brovkin, V., Raddatz, T., Reick, C. H., Claussen, M., and Gayler, V.: Global biogeophysical interactions between forest and climate, Geophys. Res. Lett., 36, L07405, doi:10.1029/2009GL037543, 2009.

Burke, E. J. and Brown, S. J.: Evaluating Uncertainties in the Projection of Future Drought, J. Hydrometeorol., 9, 292–299, doi:10.1175/2007JHM929.1, 2008.

Ciais, P., Reichstein, M., Viovy, N., Granier, A., Ogee, J., Allard, V., Aubinet, M., Buchmann, N., Bernhofer, C., Carrara, A., Chevallier, F., De Noblet, N., Friend, A. D., Friedlingstein, P., Grunwald, T., Heinesch, B., Keronen, P., Knohl, A., Krinner, G., Loustau, D., Manca, G., Matteucci, G., Miglietta, F., Ourcival, J. M., Papale, D., Pilegaard, K., Rambal, S., Seufert, G., Soussana, J. F., Sanz, M. J., Schulze, E. D., Vesala, T., and Valentini, R.: Europe-wide reduction in primary productivity caused by the heat and drought in 2003, Nature, 437, 529–533, 2005.

Clenciala, E., Kucera, J., Ryan, M., G., and Lindroth, A.: Water flux in boreal forest during two hydrologically contrasting years; species specific regulation of canopy conductance and transpiration, Ann. For. Sci., 55, 47–61, 1998.

Dai, A.: Increasing drought under global warming in observations and models, Nature Clim. Change, 3, 52–58, 2013.

Dale, V. H., Joyce, L. A., McNulty, S., Neilson, R. P., Ayres, M. P., Flannigan, M. D., Hanson, P. J., Irland, L. C., Lugo, A. E., Peterson, C. J., Simberloff, D., Swanson, F. J., Stocks, B. J., and Michael Wotton, B.: Climate change and forest disturbances, BioScience, 51, 723–734, doi:10.1641/0006-3568(2001)051[0723:CCAFD]2.0.CO;2, 2001.

Dee, D. P., Uppala, S. M., Simmons, A. J., Berrisford, P., Poli, P., Kobayashi, S., Andrae, U., Balmaseda, M. A., Balsamo, G., Bauer, P., Bechtold, P., Beljaars, A. C. M., van de Berg, L., Bidlot, J., Bormann, N., Delsol, C., Dragani, R., Fuentes, M., Geer, A. J., Haimberger, L., Healy, S. B., Hersbach, H., Hólm, E. V., Isaksen, L., Kållberg, P., Köhler, M., Matricardi, M., McNally, A. P., Monge-Sanz, B. M., Morcrette, J. J., Park, B. K., Peubey, C., de Rosnay, P., Tavolato, C., Thépaut, J. N., and Vitart, F.: The ERA-Interim reanalysis: configuration and performance of the data assimilation system, Q. J. Roy. Meteor. Soc., 137, 553–597, doi:10.1002/qj.828, 2011.

Drebs, A., Nordlund, A., Karlsson, P., Helminen, J., and Rissanen, P.: Climatological statistics of Finland 1971–2000, in: Climatological Statistics of Finland 2001, Finnish Meteorological Institute, Helsinki, 2002.

Dümenil, L. and Todini, E.: A rainfall–runoff scheme for use in the Hamburg climate model, in: Advances in Theoretical Hydrology – a Tribute to James Dooge, European Geophysical Society Series on Hydrological Sciences, edited by: O'Kane, J. P., Elsevier Science, Amsterdam, the Netherlands, 129–157, 1992.

Dunne, K. and Willmott, C. J.: Global distribution of plant-extractable water capacity of soil, Int. J. Climatol., 16, 841–859, 1996.

Edwards, D. C. and McKee, T. B.: Characteristics of 20th century drought in the United States at multiple time scales. Climatology Report 97-2, Department of Atmospheric Science, Colorado State University, Fort Collins, Colorado, 1997.

European Environment Agency: CLC2006 technical guidelines, EEA Technical Report No. 17, Copenhagen, 2007.

FAO/UNESCO: Soil Map of the World, UNESCO, Paris, 1971–1981.

Finnish Statistical Yearbook of Forestry 2012, The Finnish Forest Research Institute, Helsinki, Finland, 454 pp., 2012.

Gao, Y., Weiher, S., Markkanen, T., Pietikäinen, J.-P., Gregow, H., Henttonen, H. M., Jacob, D., and Laaksonen, A.: Implementation of the CORINE land use classification in the regional climate model REMO, Boreal Environ. Res., 20, 261–282, 2015.

Gimbel, K. F., Felsmann, K., Baudis, M., Puhlmann, H., Gessler, A., Bruelheide, H., Kayler, Z., Ellerbrock, R. H., Ulrich, A., Welk, E., and Weiler, M.: Drought in forest understory ecosystems – a novel rainfall reduction experiment, Biogeosciences, 12, 961–975, doi:10.5194/bg-12-961-2015, 2015.

Granier, A., Bréda, N., Biron, P., and Villette, S.: A lumped water balance model to evaluate duration and intensity of drought constraints in forest stands, Ecol. Model., 116, 269–283, doi:10.1016/S0304-3800(98)00205-1, 1999.

Granier, A., Reichstein, M., Bréda, N., Janssens, I. A., Falge, E., Ciais, P., Grünwald, T., Aubinet, M., Berbigier, P., Bernhofer, C., Buchmann, N., Facini, O., Grassi, G., Heinesch, B., Ilvesniemi, H., Keronen, P., Knohl, A., Köstner, B., Lagergren, F., Lindroth, A., Longdoz, B., Loustau, D., Mateus, J., Montagnani, L., Nys, C., Moors, E., Papale, D., Peiffer, M., Pilegaard, K., Pita, G., Pumpanen, J., Rambal, S., Rebmann, C., Rodrigues, A., Seufert, G., Tenhunen, J., Vesala, T., and Wang, Q.: Evidence for soil water control on carbon and water dynamics in European forests during the extremely dry year: 2003, Agr. Forest Meteorol., 143, 123–145, doi:10.1016/j.agrformet.2006.12.004, 2007.

Grossiord, C., Granier, A., Gessler, A., Jucker, T., and Bonal, D.: Does drought influence the relationship between biodiversity and ecosystem functioning in boreal forests?, Ecosystems, 17, 394–404, doi:10.1007/s10021-013-9729-1, 2014.

Grünzweig, J. M., Lin, T., Rotenberg, E., Schwartz, A., and Yakir, D.: Carbon sequestration in arid-land forest, Glob. Change Biol., 9, 791–799, doi:10.1046/j.1365-2486.2003.00612.x, 2003.

Guttman, N. B.: On the sensitivity of sample L moments to sample size, J. Climate, 7, 1026–1029, doi:10.1175/1520-0442(1994)007<1026:OTSOSL>2.0.CO;2, 1994.

Guttman, N. B.: Accepting the standardized precipitation index: a calculation algorithm, J. Am. Water Resour. As., 35, 311–322, 1999.

Hagemann, S.: An Improved Land Surface Parameter Dataset for Global and Regional Climate Models, Max Planck Institute for Meteorology, Hamburg, 2002.

Hagemann, S. and Stacke, T.: Impact of the soil hydrology scheme on simulated soil moisture memory, Clim. Dynam., 44, 1731–1750, doi:10.1007/s00382-014-2221-6, 2015.

Hain, C. R., Crow, W. T., Mecikalski, J. R., Anderson, M. C., and Holmes, T.: An intercomparison of available soil moisture estimates from thermal infrared and passive microwave remote sensing and land surface modeling, J. Geophys. Res.-Atmos., 116, D15107, doi:10.1029/2011JD015633, 2011.

Hayes, M., Svoboda, M., Wall, N., and Widhalm, M.: The Lincoln declaration on drought indices: universal meteorological drought index recommended, B. Am. Meteorol. Soc., 92, 485–488, doi:10.1175/2010BAMS3103.1, 2011.

Heim, R. R.: A review of twentieth-century drought indices used in the United States, B. Am. Meteorol. Soc., 83, 1149–1165, doi:10.1175/1520-0477(2002)083<1149:AROTDI>2.3.CO;2, 2002.

Hillel, D.: Environmental Soil Physics, Academic Press, San Diego, 1998.

IPCC: Managing the Risks of Extreme Events and Disasters to Advance Climate Change Adaptation. A Special Report of Working Groups I and II of the Intergovernmental Panel on Climate Change, edited by: Field, C. B., Barros, V., Stocker, T. F., Qin, D., Dokken, D. J., Ebi, K. L., Mastrandrea, M. D., Mach, K. J., Plattner, G.-K., Allen, S. K., Tignor, M., and Midgley, P. M., Cambridge University Press, Cambridge, UK, and New York, NY, USA, 582 pp., 2012.

Irvine, J., Perks, M. P., Magnani, F., and Grace, J.: The response of Pinus sylvestris to drought: stomatal control of transpiration and hydraulic conductance, Tree Physiol., 18, 393–402, doi:10.1093/treephys/18.6.393, 1998.

Jacob, D.: A note to the simulation of the annual and inter-annual variability of the water budget over the Baltic Sea drainage basin, Meteorol. Atmos. Phys., 77, 61–73, doi:10.1007/s007030170017, 2001.

Jacob, D. and Podzun, R.: Sensitivity studies with the regional climate model REMO, Meteorol. Atmos. Phys., 63, 119–129, doi:10.1007/BF01025368, 1997.

Krishnan, P., Black, T. A., Grant, N. J., Barr, A. G., Hogg, E. T. H., Jassal, R. S., and Morgenstern, K.: Impact of changing soil moisture distribution on net ecosystem productivity of a boreal aspen forest during and following drought, Agr. Forest Meteorol., 139, 208–223, 2006.

Lagergren, F. and Lindroth, A.: Transpiration response to soil moisture in pine and spruce trees in Sweden, Agr. Forest Meteorol., 112, 67–85, doi:10.1016/S0168-1923(02)00060-6, 2002.

Law, B. E., Falge, E., Gu, L., Baldocchi, D. D., Bakwin, P., Berbigier, P., Davis, K., Dolman, A. J., Falk, M., Fuentes, J. D., Goldstein, A., Granier, A., Grelle, A., Hollinger, D., Janssens, I. A., Jarvis, P., Jensen, N. O., Katul, G., Mahli, Y., Matteucci, G., Meyers, T., Monson, R., Munger, W., Oechel, W., Olson, R., Pilegaard, K., Paw U, K. T., Thorgeirsson, H., Valentini, R., Verma, S., Vesala, T., Wilson, K., and Wofsy, S.: Environmental controls over carbon dioxide and water vapor exchange of terrestrial vegetation, Agr. Forest Meteorol., 113, 97–120, doi:10.1016/S0168-1923(02)00104-1, 2002.

Lenton, T. M., Held, H., Kriegler, E., Hall, J. W., Lucht, W., Rahmstorf, S., and Schellnhuber, H. J.: Tipping elements in the Earth's climate system, P. Natl. Acad. Sci. USA, 105, 1786–1793, doi:10.1073/pnas.0705414105, 2008.

Liu, Y. Y., Dorigo, W. A., Parinussa, R. M., de Jeu, R. A. M., Wagner, W., McCabe, M. F., Evans, J. P., and van Dijk, A. I. J. M.: Trend-preserving blending of passive and active microwave soil moisture retrievals, Remote Sens. Environ., 123, 280–297, doi:10.1016/j.rse.2012.03.014, 2012.

López-Urrea, R., Olalla, F. M. d. S., Fabeiro, C., and Moratalla, A.: An evaluation of two hourly reference evapotranspiration equations for semiarid conditions, Agr. Water Manage., 86, 277–282, doi:10.1016/j.agwat.2006.05.017, 2006.

Ma, Z., Peng, C., Zhu, Q., Chen, H., Yu, G., Li, W., Zhou, X., Wang, W., and Zhang, W.: Regional drought-induced reduction in the biomass carbon sink of Canada's boreal forests, P. Natl. Acad. Sci. USA, 109, 2423–2427, doi:10.1073/pnas.1111576109, 2012.

Maggioni, V., Anagnostou, E. N., and Reichle, R. H.: The impact of model and rainfall forcing errors on characterizing soil moisture uncertainty in land surface modeling, Hydrol. Earth Syst. Sci., 16, 3499–3515, doi:10.5194/hess-16-3499-2012, 2012.

McKee, T. B., Doeskin, N. J., and Kleist, J.: The relationship of drought frequency and duration to time scales, in: 8th Conference on Applied Climatology, Anaheim, Califonia, 179–184, 1993.

McKee, T. B., Doesken, N. J., and Kleist, J.: Drought monitoring with multiple time scales, in: Ninth Conference on Applied Climatology, Dallas, Texas, 233–236, 1995.

Mishra, A. K. and Singh, V. P.: A review of drought concepts, J. Hydrol., 391, 202–216, doi:10.1016/j.jhydrol.2010.07.012, 2010.

Muukkonen, P., Nevalainen, S., Lindgren, M., and Peltoniemi, M.: Spatial Occurrence of Drought-Associated Damages in Finnish Boreal Forests: Results from Forest Condition Monitoring and GIS Analysis, Boreal Environ. Res., 20, 172–180, 2015.

Naumann, G., Dutra, E., Barbosa, P., Pappenberger, F., Wetterhall, F., and Vogt, J. V.: Comparison of drought indicators derived from multiple data sets over Africa, Hydrol. Earth Syst. Sci., 18, 1625–1640, doi:10.5194/hess-18-1625-2014, 2014.

Orlowsky, B. and Seneviratne, S. I.: Elusive drought: uncertainty in observed trends and short- and long-term CMIP5 projections, Hydrol. Earth Syst. Sci., 17, 1765–1781, doi:10.5194/hess-17-1765-2013, 2013.

Päivänen, J. and Hånell, B.: Peatland Ecology and Forestry: a Sound Approach, Department of Forest Ecology, University of Helsinki, 2012.

Peng, C., Ma, Z., Lei, X., Zhu, Q., Chen, H., Wang, W., Liu, S., Li, W., Fang, X., and Zhou, X.: A drought-induced pervasive increase in tree mortality across Canada's boreal forests, Nature Clim. Change, 1, 467–471, 2011.

Quiring, S. M.: Developing objective operational definitions for monitoring drought, J. Appl. Meteorol. Clim., 48, 1217–1229, doi:10.1175/2009JAMC2088.1, 2009.

Raddatz, T. J., Reick, C. H., Knorr, W., Kattge, J., Roeckner, E., Schnur, R., Schnitzler, K. G., Wetzel, P., and Jungclaus, J.: Will the tropical land biosphere dominate the climate–carbon cycle feedback during the twenty-first century?, Clim. Dynam., 29, 565–574, doi:10.1007/s00382-007-0247-8, 2007.

Räisänen, J. and Räty, O.: Projections of daily mean temperature variability in the future: cross-validation tests with ENSEMBLES regional climate simulations, Clim. Dynam., 41, 1553–1568, doi:10.1007/s00382-012-1515-9, 2013.
Räty, O., Räisänen, J., and Ylhäisi, J.: Evaluation of delta change and bias correction methods for future daily precipitation: intermodel cross-validation using ENSEMBLES simulations, Clim. Dynam., 42, 2287–2303, doi:10.1007/s00382-014-2130-8, 2014.
Rebel, K. T., de Jeu, R. A. M., Ciais, P., Viovy, N., Piao, S. L., Kiely, G., and Dolman, A. J.: A global analysis of soil moisture derived from satellite observations and a land surface model, Hydrol. Earth Syst. Sci., 16, 833–847, doi:10.5194/hess-16-833-2012, 2012.
Roeckner, E., Arpe, K., Bengtsson, L., Christoph, M., Claussen, M., Dümenil, L., Esch, M., Giogetta, M., Schlese, U., and Schultz-Weida, U.: The Atmospheric General Circulation Model ECHAM4: Model Description and Simulation of the Present-Day Climate, Max Planck Institute for Meterology, Hamburg, 90 pp., 1996.
Schär, C., Vidale, P. L., Luthi, D., Frei, C., Haberli, C., Liniger, M. A., and Appenzeller, C.: The role of increasing temperature variability in European summer heatwaves, Nature, 427, 332–336, 2004.
Seneviratne, S. I., Corti, T., Davin, E. L., Hirschi, M., Jaeger, E. B., Lehner, I., Orlowsky, B., and Teuling, A. J.: Investigating soil moisture–climate interactions in a changing climate: a review, Earth-Sci. Rev., 99, 125–161, doi:10.1016/j.earscirev.2010.02.004, 2010.
Sergio, M. V.-S., Juan, I. L.-M., Santiago, B., Jorge, L.-L., Arturo, S.-L., José, M. G.-R., Cesar, A.-M., Enrique, M.-T., Jesús, R., Ricardo, T., Fatima, C., and Francisco, E.: Evidence of increasing drought severity caused by temperature rise in southern Europe, Environ. Res. Lett., 9, 044001, doi:10.1088/1748-9326/9/4/044001, 2014.
Sheffield, J. and Wood, E. F.: Drought: Past Problems and Future Scenarios, Earthscan, London, UK and Washington, DC, USA, 2011.
Simmons, A., Uppala, S., Dee, D., and Kobayashi, S.: ERA-Interim: new ECMWF reanalysis products from 1989 onwards, ECMWF Newsletter, 110, 25–35, 2007.
Sivakumar, M. V. K., Motha, R. P., Wilhite, D. A., and Wood, D. A.: Agricultural drought indices, in: Proceedings of the WMO/UNISDR Expert Group Meeting on Agricultural Drought Indice, 2–4 June 2010, Murcia, Spain, World Meteorological Organization, Geneva, Switzerland, AGM-11, WMO/TD No. 1572; WAOB-2011, 197 pp., 2011.
Stevens, B., Giorgetta, M., Esch, M., Mauritsen, T., Crueger, T., Rast, S., Salzmann, M., Schmidt, H., Bader, J., Block, K., Brokopf, R., Fast, I., Kinne, S., Kornblueh, L., Lohmann, U.,

Pincus, R., Reichler, T., and Roeckner, E.: Atmospheric component of the MPI-M Earth System Model: ECHAM6, Journal of Advances in Modeling Earth Systems, 5, 146–172, doi:10.1002/jame.20015, 2013.

Tallaksen, L. M. and Van Lanen, H. A. J.: Hydrological Drought: Processes and Estimation Methods for Streamflow and Groundwater, Elsevier Science B.V., the Netherlands, 2004.

Thum, T., Aalto, T., Laurila, T., Aurela, M., Lindroth, A., and Vesala, T.: Assessing seasonality of biochemical CO_2 exchange model parameters from micrometeorological flux observations at boreal coniferous forest, Biogeosciences, 5, 1625–1639, doi:10.5194/bg-5-1625-2008, 2008.

Tikkanen, M.: The Physical Geography of Fennoscandia, edited by: Seppälä, M., Oxford University Press, Oxford, 2005.

Törmä, M., Markkanen, T., Hatunen, S., Härmä, P., Mattila, O.-P., and Arslan, A. N.: Assessment of land-cover data for land-surface modelling in regional climate studies, Boreal Environ. Res., 20, 243–260, 2015.

US Geological Survey: Global Land Cover Characteristics Data Base version 2.0, US Geological Survey, Reston, USA, 2001.

Van Loon, A. F. and Van Lanen, H. A. J.: A process-based typology of hydrological drought, Hydrol. Earth Syst. Sci., 16, 1915–1946, doi:10.5194/hess-16-1915-2012, 2012.

Veit, B., Lukas, G., and Kerstin, S.: Towards pan-European drought risk maps: quantifying the link between drought indices and reported drought impacts, Environ. Res. Lett., 10, 014008, doi:10.1088/1748-9326/10/1/014008, 2015.

Ventura, F., Spano, D., Duce, P., and Snyder, R. L.: An evaluation of common evapotranspiration equations, Irrigation Sci., 18, 163–170, doi:10.1007/s002710050058, 1999.

Vesala, T., Suni, T., Rannik, Ü., Keronen, P., Markkanen, T., Sevanto, S., Grönholm, T., Smolander, S., Kulmala, M., Ilvesniemi, H., Ojansuu, R., Uotila, A., Levula, J., Mäkelä, A., Pumpanen, J., Kolari, P., Kulmala, L., Altimir, N., Berninger, F., Nikinmaa, E., and Hari, P.: Effect of thinning on surface fluxes in a boreal forest, Global Biogeochem. Cy., 19, GB2001, doi:10.1029/2004GB002316, 2005.

Vicente-Serrano, S. M., Beguería, S., and López-Moreno, J. I.: A multiscalar drought index sensitive to global warming: the standardized precipitation evapotranspiration index, J. Climate, 23, 1696–1718, doi:10.1175/2009JCLI2909.1, 2010.

Welp, L. R., Randerson, J. T., and Liu, H. P.: The sensitivity of carbon fluxes to spring warming and summer drought depends on plant functional type in boreal forest ecosystems, Agr. Forest Meteorol., 147, 172–185, doi:10.1016/j.agrformet.2007.07.010, 2007.
World Meteorological Organization: Standardized Precipitation Index User Guide, edited by: Svoboda, M., Hayes, M., and Wood, D., WMO-No. 1090, 16 pp., Geneva, Switzerland, 2012.
Wu, H., Svoboda, M. D., Hayes, M. J., Wilhite, D. A., and Wen, F.: Appropriate application of the standardized precipitation index in arid locations and dry seasons, Int. J. Climatol., 27, 65–79, doi:10.1002/joc.1371, 2007.

HESSD
12, 8091–8129, 2015

Table 1. Characteristics of the three micrometeorological sites. The plant functional types and the soil types in the JSBACH site simulations corresponding to observed tree species and soil types at the three sites are shown in brackets.

Site	Location	Period	Main Tree Specie	Soil Type	Analyzed Measurement Depth of soil moisture (cm)	Measurement Technique for soil moisture	References
Hyytiälä	61°51′ N, 24°18′ E	1999–2009	Scots Pine (Conifers)	Haplicpodzol (Mineral)	−5 to −23; −23 to −60	TDR	Vesala et al. (2005)
Sodankylä	67°21′ N, 26°38′ E	2001–2008	Scots Pine (Conifers)	Sandy Podzol (Mineral)	−10, −20, −30 (averaged)	ThetaProbe	Thum et al. (2008)
Kenttärova	67°59′ N, 24°15′ E	2008–2010	Norway Spruce (Conifers)	Podzol (Mineral)	−10	ThetaProbe	Aurela et al. (2015)

HESSD
12, 8091–8129, 2015

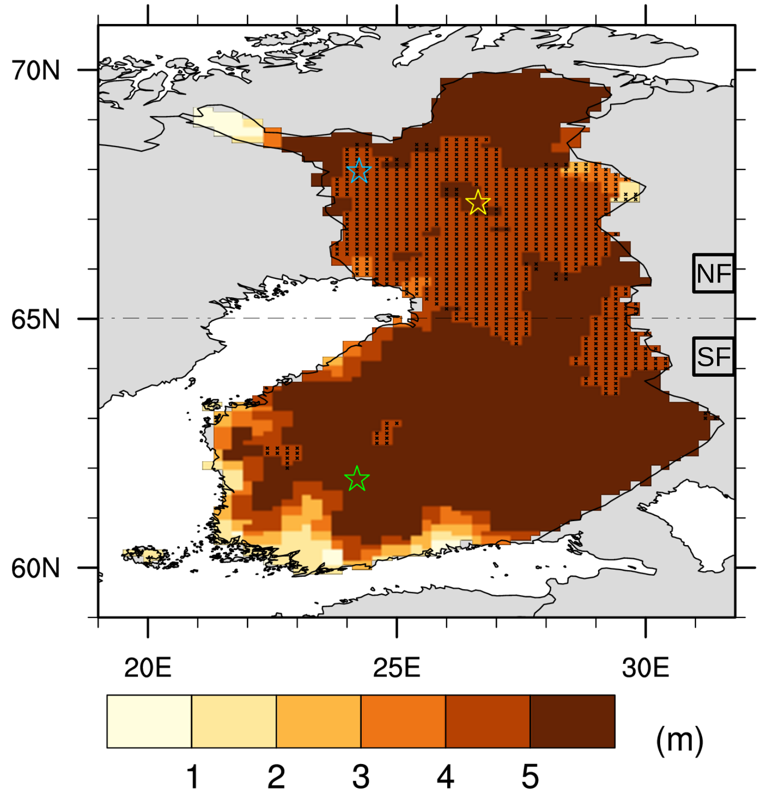

Figure 1. Soil depth and soil type distributions in JSBACH over Finland (peatland area – dotted area; mineral soil area – area without dots). Northern (NF) and southern Finland (SF) are divided at the 65° N latitude. The location of the three ecosystem sites used in this study are marked as stars on the map (Green–Hyytiälä; Yellow–Sodankylä; Blue–Kenttärova).

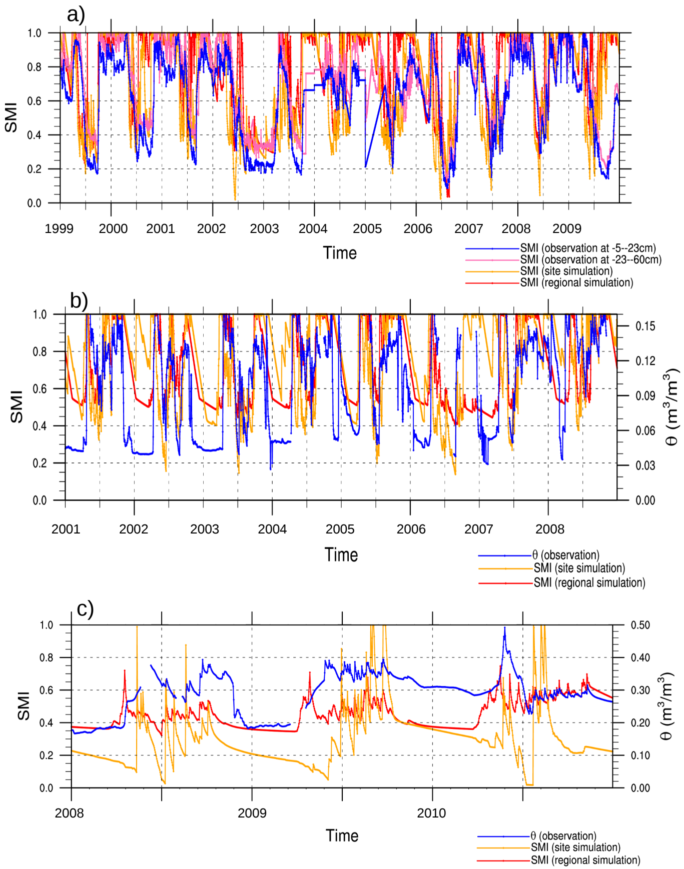

Figure 2. Soil moisture dynamics at the three micrometeorological sites: **(a)** Hyytiälä, **(b)** Sodankylä and **(c)** Kenttärova, comparing results from regional (the model gridboxs where the sites are located) and site JSBACH simulations with observations. The volumetric soil moisture (θ) is shown for the Sodankylä and Kenttärova sites.

HESSD
12, 8091–8129, 2015

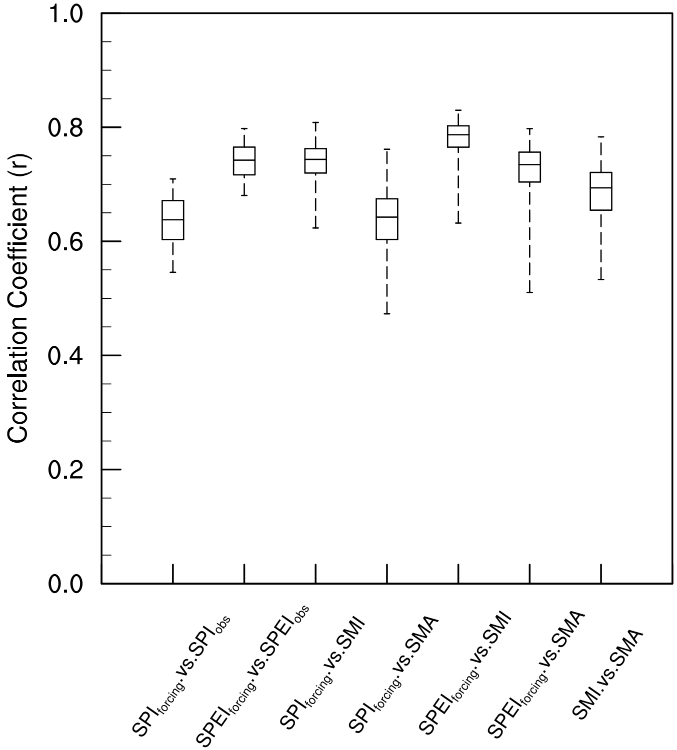

Figure 3. Percentiles of the time correlation coefficients across the gridboxes over Finland. The time correlations over the study period between the SPIs and SPEIs derived from the JSBACH forcing data and the observational dataset ($SPI_{forcing}$ vs. SPI_{obs}, $SPEI_{forcing}$ vs. $SPEI_{obs}$), as well as the time correlations between SPI, SPEI calculated with the JSBACH forcing data and SMI, SMA calculated with the JSBACH simulated soil moisture ($SPI_{forcing}$ vs. SMI, $SPI_{forcing}$ vs. SMA, $SPEI_{forcing}$ vs. SMI, $SPEI_{forcing}$ vs. SMA) are investigated. Dashed lines extend from 5th to 95th percentile of the correlation coefficients over Finland, boxes extend from 25th to 75th percentile and middle horizontal lines within each box are the medians.

HESSD
12, 8091–8129, 2015

Assessing various drought indicators in boreal forests

Y. Gao et al.

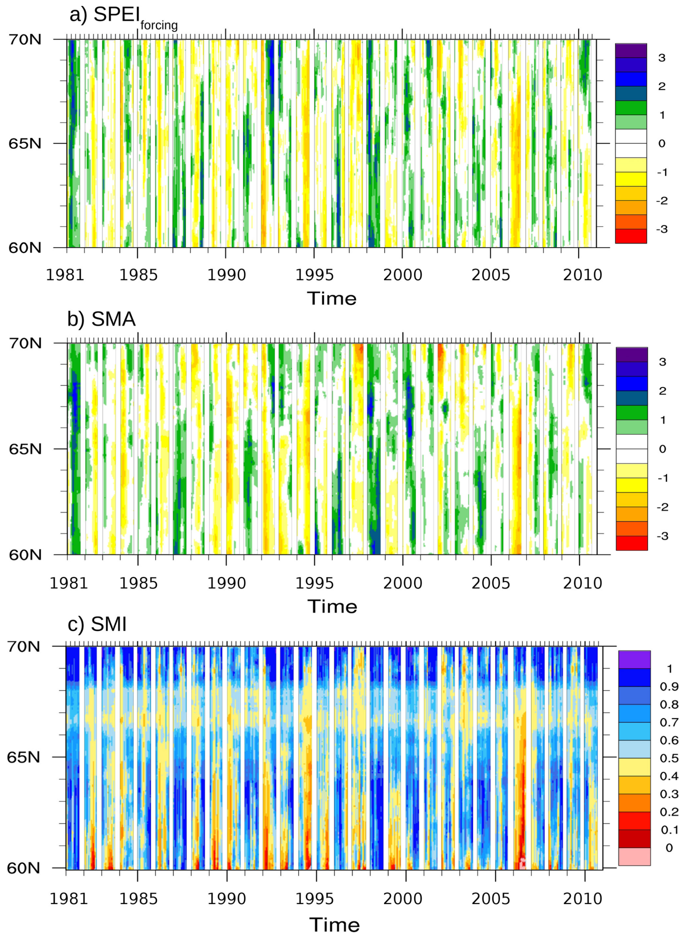

Figure 4. Latitude–time transections of **(a)** SPEI$_{forcing}$, **(b)** SMA and **(c)** SMI over Finland in the study period (the summer months (June, July, August) in 1981–2010).

HESSD
12, 8091–8129, 2015

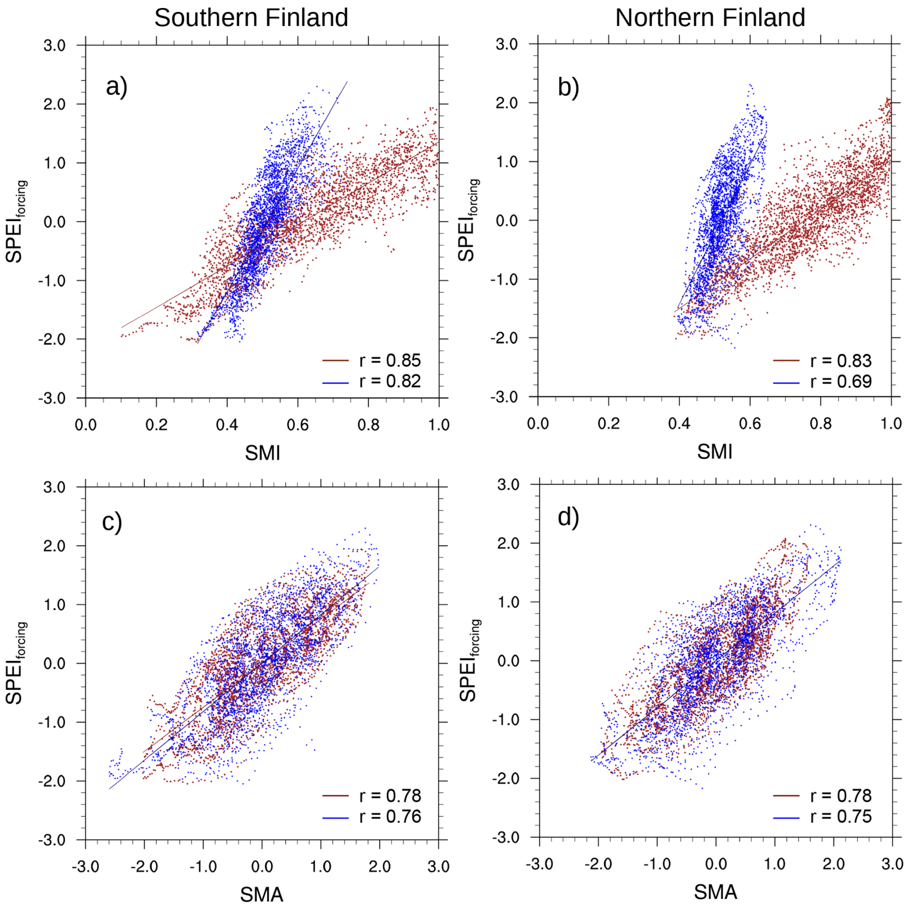

Figure 5. Time correlations over the study period between SPEI$_{forcing}$ and SMI **(a, b)**, SPEI$_{forcing}$ and SMA **(c, d)** with the spatial means over the mineral soil areas (brown) and the peat soil areas (blue) in southern Finland (left column) and northern Finland (right column), respectively.

HESSD
12, 8091–8129, 2015

Assessing various drought indicators in boreal forests

Y. Gao et al.

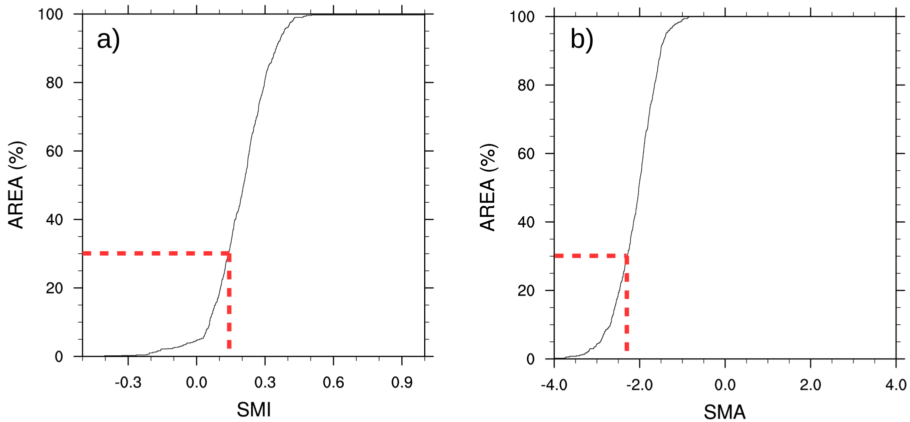

Figure 6. Cumulative area distribution of the **(a)** SMI and **(b)** SMA over southern Finland in the driest 28 day period of southern Finland in 2006 (i.e. the driest day of 28 day running means of the regionally averaged SMI and SMA over southern Finland). The red dashed lines indicate the corresponding SMI and SMA values at which 30 % of the area is affected by the Extreme Drought that affects Forest health (EDF).

HESSD
12, 8091–8129, 2015

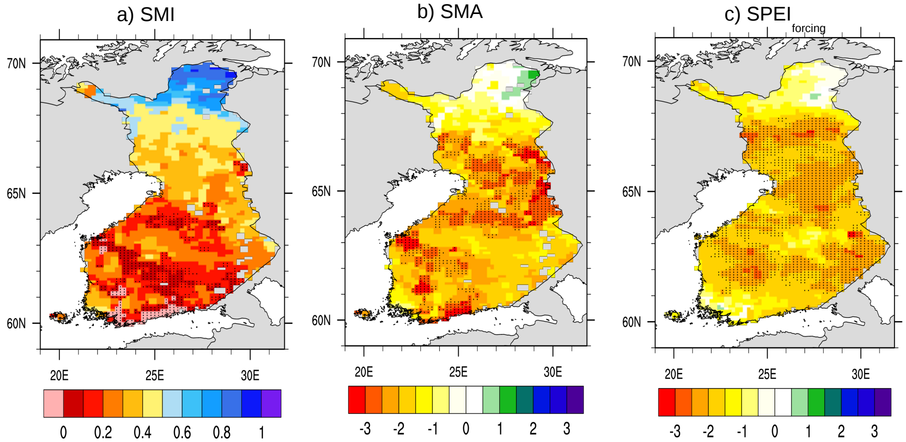

Figure 7. The **(a)** SMI, **(b)** SMA, **(c)** SPEI$_{forcing}$ in the driest 28 day period of southern Finland in 2006. The dotted areas are under the derived thresholds for EDF.

HESSD
12, 8091–8129, 2015

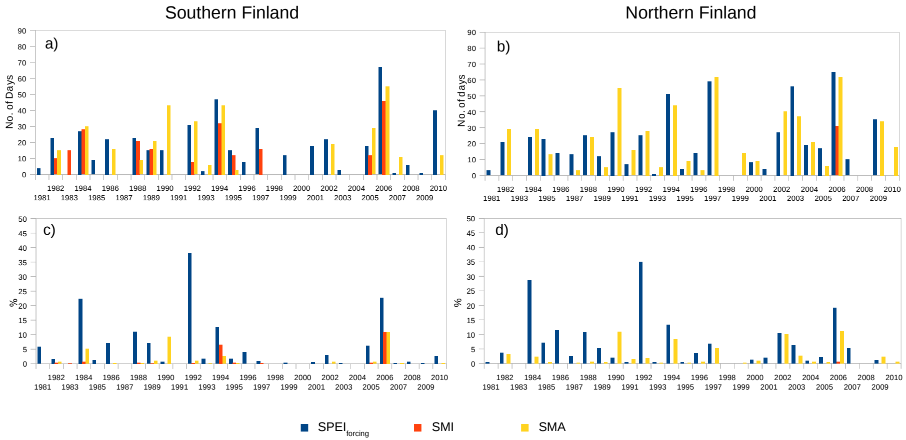

Figure 8. The summer drought periods **(a, b)** and the mean fractional areas affected by drought in these periods **(c, d)** induced by EDF events that are indicated by SMI, SMA and SPEI$_{forcing}$ for southern Finland (left column) and northern Finland (right column) in the study period (note that areas with shallow soil (soil depth < 3 m) are excluded).

HESSD

12, 8091–8129, 2015

Assessing various drought indicators in boreal forests

Y. Gao et al.